9th World Conference on Experimental Heat Transfer, Fluid Mechanics and Thermodynamics
12-15 June, 2017, Iguazu Falls, Brazil

SIMULTANEOUS CAPACITIVE PROBE AND PLANAR LASER-INDUCED FLUORESCENCE MEASUREMENTS IN DOWNWARDS GAS–LIQUID ANNULAR FLOW

Steven Lecompte*
Department of Flow, Heat and Combustion Mechanics, Ghent University, Sint-Pietersnieuwstraat 41, 9000 Ghent, Belgium
*steven.lecompte@ugent.be
Jae S. An
Clean Energy Processes (CEP) Laboratory, Department of Chemical Engineering, Imperial College London, London SW7 2AZ, United Kingdom
Alexandros Charogiannis
Clean Energy Processes (CEP) Laboratory, Department of Chemical Engineering, Imperial College London, London SW7 2AZ, United Kingdom
Michel De Paepe
Department of Flow, Heat and Combustion Mechanics, Ghent University, Sint-Pietersnieuwstraat 41, 9000 Ghent, Belgium
Christos N. Markides
Clean Energy Processes (CEP) Laboratory, Department of Chemical Engineering, Imperial College London, London SW7 2AZ, United Kingdom

Keywords: flow meter, capacitive probe, optical, laser-induced fluorescence, PLIF, annular flow

Abstract. Various experimental techniques are available to analyse two-phase flows. The measurement concept and the applicability can however vary greatly. Prime examples from the opposite spectrum are planar laser-induced measurements (PLIF) versus capacitive probes. PLIF is an optical technique, it is non-intrusive but optical access is necessary. PLIF based measurements are known for their high temporal and spatial resolution but require a costly set-up. In contrast, the capacitive probe is another non-intrusive technique but doesn't require optical access. It is fairly easy to set up, robust, and is cheap to construct. To rigorously compare both techniques, simultaneous PLIF and capacitive probe measurements are made in this work. As the void fraction is one of the key parameters to classify flow regimes, both techniques are compared on the determination of the void fraction. This is done for a limited set of six annular flows. The experiments were performed in a downward annular-flow facility with demineralized water - air as working medium. The first results indicate that both techniques give similar volume averaged void fractions. The mean absolute percentage error and the maximum relative error between both techniques are 0.30% and 0.54%, respectively. The PLIF measurements confirm however to have a better spatial resolution.

1. INTRODUCTION

The void fraction is one of the key parameters to characterize two-phase flow. As such several experimental methods to determine the void fraction have been proposed. These comprise intrusive methods (e.g. wire mesh tomography) and non-intrusive methods. The non-intrusive methods have the benefit that there is definitely no effect on the investigated flow. In this group, two large categories of measurement techniques are found, either optical or electromagnetic. Optical techniques require transparent tubing, for example glass or plastic, and are therefore only applicable to low pressures and temperatures. They are typically complex and costly to set up. Electromagnetic void fraction sensors are frequently used because they are easy to implement, have a low cost and no direct optical access is required. The group of electromagnetic probes consists of resistive and capacitive sensors. As the name suggests, the first detects changes in resistance and the second changes in capacitance. Capacitive sensors are used in non-conductive flows but they are also applicable to conductive flows with an adapted measuring circuit (Demori *et al.*, 2010). The main drawback of electromagnetic probes is that the spatial resolution is low. In addition calibration is necessary as explained in the paragraph below.

The measured capacitance in capacitive probes does not vary linearly with the void fraction (De Kerpel *et al.*, 2014). This is due to the curvature of the electrodes. This curvature imposes a non-homogeneous electric field and the capacitance will also change based on the spatial distribution of the liquid-vapour phase. Two main methods are conventionally used to calibrate the probe. The first uses Finite Element Simulations (FEM) to determine the void fraction-capacitance relation. For each flow regime a simplified liquid-vapour structure is assumed and subsequently simulated. A second technique uses inserts to mimic the liquid-vapour phase structure. The drawback is that inserts are

severely limited by their shapes and size. An additional challenge is that the inserts need to have the similar dielectric constants as the phases.

In this work, Planar Laser Induced Florescence (PLIF) measurements are made with concurrent capacitance measurements. The principal aim is to investigate both techniques for determining the average volume void fraction. In addition, as both measurement techniques are used at the same time, a direct comparison in terms of temporal and spatial resolution is possible. The acquired measurements are highly unique and can be used as a reference calibration dataset in future works.

2. EXPERIMENTAL METHODS

2.1. Flow facility

The experiments were performed in a downward annular-flow facility at Imperial College London known as DAFLOF. The main test section of this facility comprises a straight vertical pipe with an inner diameter of 32.4 mm and a total measurement length of 5.0 m, constructed from fluorinated ethylene propylene (FEP) in order to match the refractive index of water (1.33). Deionised water with a small addition of Rhodamine dye (8 mg/L) was used as the working liquid phase. A schematic of the experimental arrangement is shown in Fig. 1(a).

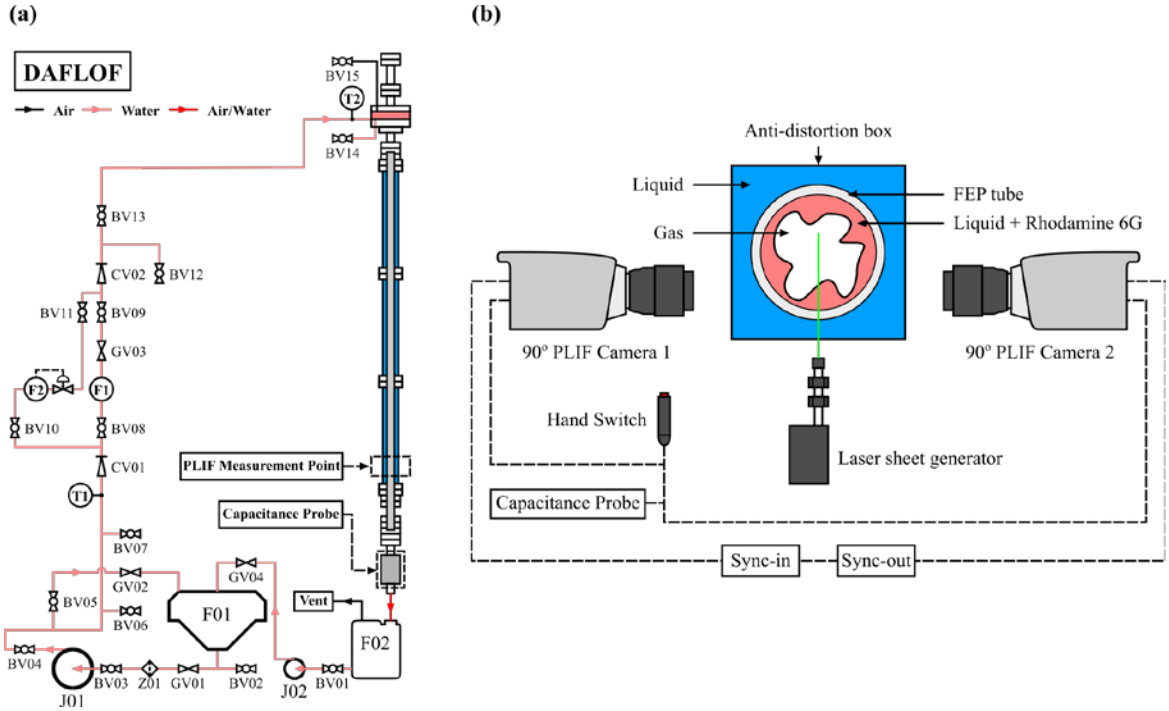

Figure 1. (a) Schematic diagram of the DAFLOF facility, (b) Illustration of the experimental configuration.

The liquid was circulated in a close-loop by a variable speed pump and introduced into the test section via a conical injector. The pipe was enclosed in a Perspex box filled with water to minimize the optical distortions caused by the cylindrical geometry of the pipe. Experiments were performed over a range of superficial gas velocities, V_g, from 0 to 39 m/s, and liquid Reynolds numbers, Re_L, from 150 to 1350. Here, $Re_L = Q/\pi dv$, where Q is volumetric liquid flow rate and v is kinematic viscosity of liquid. In total six annular flow regimes are studied. The boundary conditions for the different runs can be found in Table 1.

Table 1. Conditions for the different experimental runs.

Experimental run	Volumetric flow-rate [L/min]	Liquid temperature [°C]
1	3.63	24.5
2	5.00	24.5
3	6.79	24.5
4	8.32	24.5
5	1.67	23.5
6	0.83	23.5

2.2. Planar Laser Induced Fluorescent (PLIF)

The PLIF optics was set-up approximately 125 *L/D* downstream of the liquid injector. The fluorescent dye (Rhodamine 6G), which was seeded into the working fluid, was excited by a 2D laser sheet (λ = 510.6 nm, τ = 0.4 mm) that was produced with a Cu-vapour laser (LS20-10, Oxford Lasers Ltd) with dedicated sheet optics. A high-speed camera was positioned on either side of the excitation plane, and both cameras were aligned 90° to the illumination plane. The PLIF cameras were equipped with Sigma 105 mm f/2.8 macro lenses and 540 nm long-pass optical filters. Prior to the experiments, a graticule correction technique was employed to assist in the alignment of the optics, and to correct for perspective distortions in the raw PLIF images (Charogiannis et al., 2015). The graticule was positioned within the illumination plane and immersed in the working fluid. Images of the target were taken by both cameras. The target consisted of a 2-D pattern of squares (1 mm × 1 mm) with a separation of 1 mm between each square. A transformation was then obtained by linear correspondence of the coordinates of several squares in both images. The spatial resolution was determined to be 25 μm/pixel. For each experimental run, the PLIF images were collected at 5000 Hz, which corresponded to a sequence of 13000 recorded frames and a sampling time of 2.6 s. One conventional method of processing the PLIF images consists of identifying the position of the boundaries of the illuminated area based on a brightness threshold method, as described in detail in Farias *et al*. (2012), Schubring *et al*. (2010) and Zadrazil *et al*. (2014). For this study, the gas-liquid and the solid-liquid interfaces were located via the maximum gradient approach implemented by Charogiannis et al. (2015).

2.3. Capacitive probe

The capacitive sensor consists of two electrodes; both with an angle of 100° and a length of 16 mm. Around these electrodes two guard electrodes are placed to have a more uniform electric field (Reinicke and Mewes, 1997). The construction of the sensor is provided in Fig. 2. Flexible circuit material (R/Flex® 3000 from Rogers Corporations) was used to form the inner tube wall of the sensor. The electrodes were etched out of the copper cladding on this circuit material. The thickness of the dielectric layer is 50 μm ± 12.5%, it has an electrical resistance of 10^{12} MΩ/cm and its dielectric constant is 2.9 at 23 °C. After the electrodes were etched on the circuit material they were glued in PVC parts, which provide the structural strength. These PVC parts are then placed into a stainless steel cylindrical casing, and the annular gap between the PVC and the casing are filled with an epoxy resin. Note that the casing is not shown in Fig. 2.

The capacitance between the electrodes is measured using a transducer which was made in-house. The transducer design is based on the one proposed by Yang *et al.*, 2001. The output of the transducer is a voltage between 0 and 10 V. The sensitivity of the transducer is 1.16 V/pF and the output accuracy is 4 mV. The voltage is logged with a DAQ system. For each measurement the capacitance time trace is acquired at a sample frequency of 2 kHz.

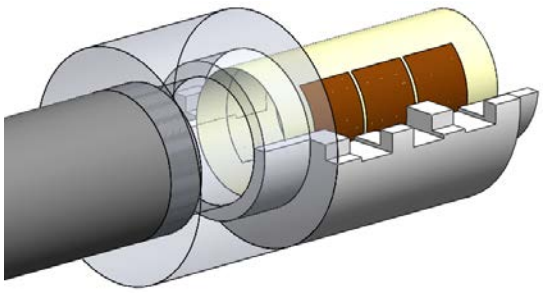

Figure 2. Overview of the capacitive probe construction.

3. CALIBRATION OF THE CAPACITIVE PROBE

A calibration procedure is required to relate the capacitance value to the void fraction. The calibration method used is based on numerical methods (i.e. FEM simulations). Details about the calibration procedure can be found in the work of De Kerpel *et al.*, 2013. The specific procedure used is shortly outlined in this section.

First, the flow structure of the annular flow is simplified by assuming two concentric circles in which between the liquid flows. Note that this void fraction thus defines a 3D time- and volume-averaged value. The dielectric constant for the air was set to 1 and the dielectric constant for the liquid phase was set to 80.1 according to Fernández *et al.*, 1995. For the FEP and the PVC material the dielectric constant is taken as 3.5 (Ott, 2009) and 2.1 (Drobny, 2001), respectively. The resulting electric potential distribution for an annular flow with a thickness of 1.62 mm is shown in Fig. 3. Note that the gradient of the electric potential in between the electrodes is very consistent. This is due to the choice of electrodes with an angle of 100° which clearly benefits the homogeneity of the electric field. As a result, the void fraction and the capacitance will approach a linear relation.

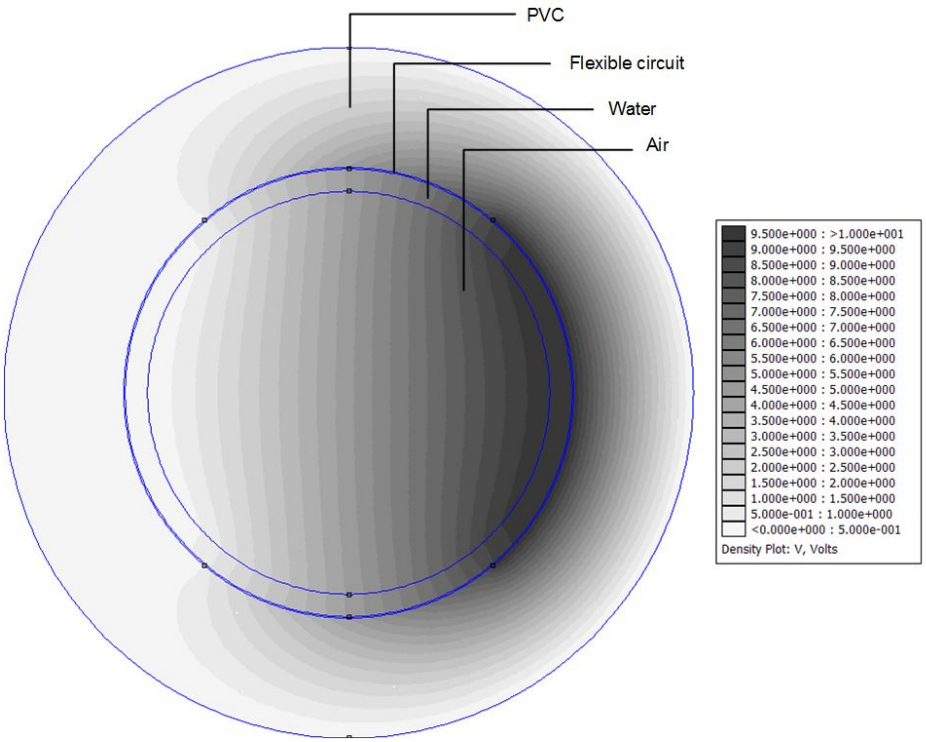

Figure 3. FEM calibration curve relating void fraction and capacitance.

The FEM simulation is now repeated for 20 geometrically evenly spaced steps between void fraction 0 and 1. The result of this calculation can be found in Fig. 4. The capacitance is normalized between its minimum (void fraction 0) and maximum value (void fraction 1) as given in Eq 1.

$$C_{nom} = \frac{C - C_{voidfraction1}}{C_{voidfraction0}} \tag{1}$$

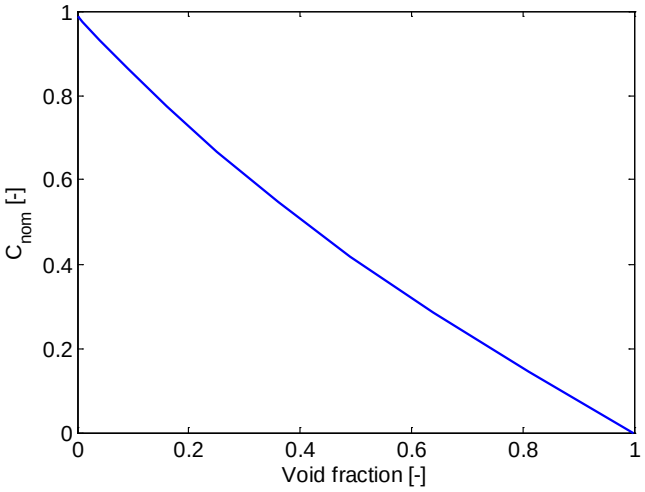

Figure 4. FEM calibration curve relating void fraction and capacitance.

As expected, the relation between void fraction and normalized capacitance is highly linear. This calibration curve can effectively be used to determine a volume averaged void fraction from the measured nominal capacitance.

Note that the measured voltage will depend linearly on the capacitance. Therefore, to determine the nominal capacitance from the measurements, it is necessary to define the calibration voltage for both void fraction zero and one. These calibration values for the probe are given in Table 2. Note that run 5 and 6 were done on a different day necessitating a new calibration of the probe.

Table 2. Conditions for the different experimental runs.

Experimental run	Calibration voltage void fraction 0 [V]	Calibration voltage void fraction 1 [V]
1,2,3,4	10.392	0.0033
5,6	10.217	0.0128

4. RESULTS

The principal goal of this work is a comparison of the void fraction determined from both the PLIF and the capacitive probe. Starting with the capacitive probe, the raw nominal capacitance is shown in Fig. 5. To convert the nominal capacitance to a void fraction, the calibration curve from Fig. 4 is used. The corresponding image, taking into account the distance between the two measurements, is shown in Fig. 6. The wave pattern is qualitatively clearly identifiable with both techniques.

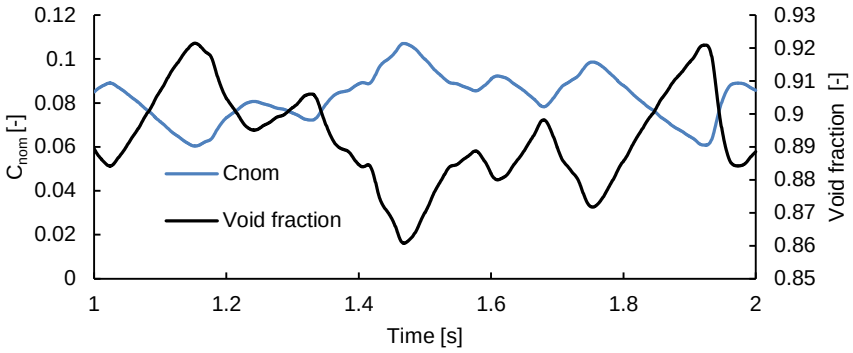

Figure 5. Excerpt of capacitive signal (Run 4) between 1 s and 2 s after triggering.

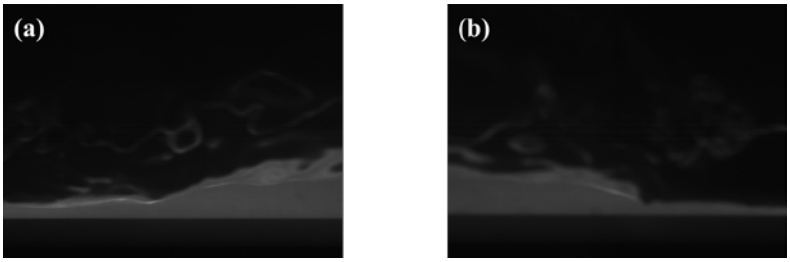

Figure 6. The same raw PLIF frame (6250) from each camera (Run 4): (a) Left-side, (b) Right-side.

To calculate a volume averaged void fraction from the PLIF images, additional assumptions are necessary about the circumferential distribution of the flow. In this work, the assumption is made that the flow is uniform in the tangential direction. The obtained void fraction is then averaged over a 2 seconds time window. Based on these assumptions, the parity plot, comparing the void fraction from both PLIF and capacitive probe, is given in Fig. 7. Qualitatively seen both techniques give similar results.

To quantify the results, the mean absolute percentage error (MAPE) is calculated. The MAPE, see Eq. 2, evaluates the deviation between the void fraction from both methods. In Eq. 2, n equals the number of measurement points and ε is the void fraction. The MAPE is 0.30% while the maximum deviation amounts to 0.54%. This can be considered a highly satisfactory result considering the assumptions taken.

$$MAPE = \frac{100}{n}\sum_{t=1}^{n}\left|\frac{\varepsilon_{probe} - \varepsilon_{PLIF}}{\varepsilon_{probe}}\right| \tag{2}$$

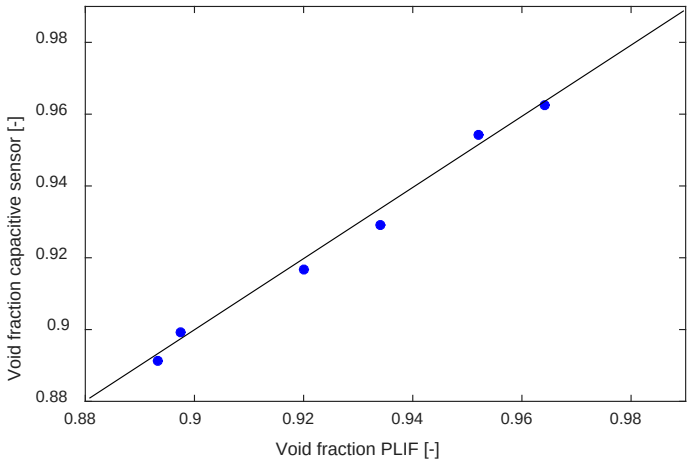

Figure 7. Comparison of the void fraction determined from both PLIF and capacitive probe for the six runs.

Capacitive probes typically have a low spatial resolution due to their construction. Long electrodes are necessary to have a measurable capacitance. Considering that an average volume void fraction is measured over the confined volume between the electrodes this leads to a low spatial resolution. This effect can also be deduced from the cumulative distribution function (CDF) of the void fraction in Fig. 8. The CDF is shown only for the six annular flows.

The PLIF measurements clearly show larger variations in void fraction compared to the capacitive probe measurements. The PLIF measurements capture the peaks of the wavy structure in detail compared to the capacitive probe measurements where these peaks are compressed due to spatial averaging. Notice however that when both measurements are averaged over a long enough time frame, the void fraction is similar. This enforces that both techniques correctly capture the flow variation, yet part of the information is not available when using the capacitive probe due to the lower spatial resolution.

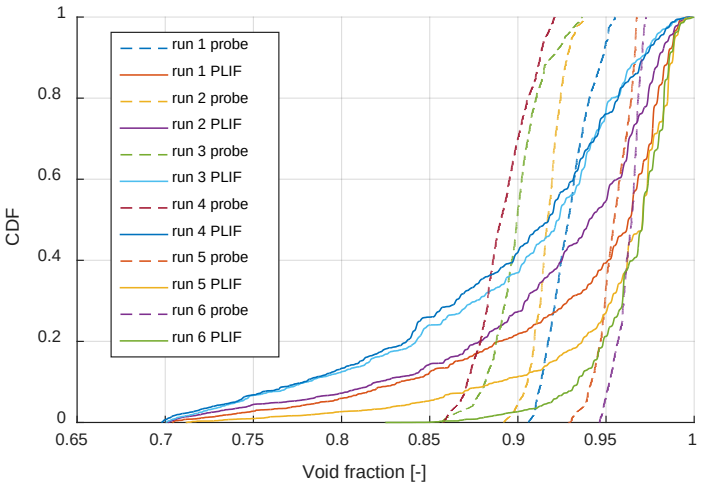

Figure 8. Cumulative distribution function (CDF) of the void fraction for the PLIF (full line) and capacitive probe measurements (dashed line) for the 6 annular flows.

4. CONCLUSION

In this work, a novel concurrent Planar Laser Induced Florescence (PLIF) and capacitive measurement was presented. A new capacitive probe was constructed for large diameter tubes. Both techniques gave similar void fraction measurements when using the processing techniques and assumptions described in this article. The maximum deviation between the void fraction is 0.54%, the mean absolute percentage error is 0.30%. Both techniques have the ability to capture qualitatively the wavy annular flow. However the details of the wavy structure will only be measurable with the PLIF method. On the other hand, the capacitive probe is cheaper, highly robust and easy to make.

In subsequent work, the unique dataset will be extended with more measurements. In particular, forced air injection and bubbly flow regimes will be investigated. Also a more in depth analysis on the flow structure, incorporating data from both techniques, will be made.

5. ACKNOWLEDGEMENTS

Steven Lecompte gratefully acknowledges the funding by Ghent University (BOF16/PDO/061) and the FWO for the international mobility grant. Data supporting this publication can be obtained on request from steven.lecompte@ugent.be.

6. REFERENCES

Charogiannis, A., An, J.S., and Markides, C.N., 2015. "A simultaneous planar laser-induced fluorescence, particle image velocimetry and particle tracking velocimetry technique for the investigation of thin liquid-film flows". *Experimental Thermal and Fluid Science*, Vol. 68, pp. 516-536.

De Kerpel, K., Ameel, B., De Schampheleire, S., T'Joen, C. Canière, H. and De Paepe, M., 2013. "Calibration of a capacitive void fraction sensor for small diameter tubes based on capacitive signal features". *Applied Thermal Engineering*, Vol. 63, pp. 77–83.

De Kerpel, K., Ameel, B., T'Joen, C. Canière, H. and De Paepe, M., 2013. "Flow regime based calibration of a capacitive void fraction sensor for small diameter tubes". *International Journal of Refrigeration*, Vol. 36, pp. 390–401.

Demori, M., Ferrari, V., Strazza, D. and Poesio, P., 2010. A capacitive sensor system for the analysis of two-phase flows of oil and conductive water". *Sensors and Actuators A: Physical*, Vol. 163, pp. 172–179.

Drobny, J.G., 2001,*Technology of Fluoropolymers*, CRC Press, Florida, pp. 31

Fernández, D.P., Mulev, Y., Goodwin, A.R.H. and Levelt Sengers J.M.H. "A Database for the Static Dielectric Constant of Water and Steam", *Journal of Physical and Chemical Reference Data*, Vol. 24, 1995, pp. 33-70.

Farias, P.S.C., Martins, F.J.W.A., Sampaio, L.E.B., Serfaty, R. and Azevedo, L.F.A., Liquid film characterization in horizontal, annular, two-phase, gas–liquid flow using time-resolved laser-induced fluorescence, *Experiments in Fluids*, Vol. 52, 2012, pp. 633–645.

Ott, H.W., 2009. *Electromagnetic Compatibility Engineering*. John Wiley & Sons, New Jersey, pp. 182

Reinicke, N. and Mewes, D., 1997. "Multielectrode capacitance sensors for the visualization of transient two-phase flows". *Experimental Thermal and Fluid Science*, Vol. 15, pp. 253–266.

Schubring, D., Ashwood, A.C., Shedd, T.B. and Hurlburt, E.T., "Planar laser-induced fluorescence (PLIF) measurements of liquid film thickness in annular flow. Part I: Methods and data", *International Journal of Multiphase Flow*, Vol. 36, 2010, pp. 815–824.

Yang, S.X. and Yang, W.Q. "A portable stray-immune capacitance meter", *Review of Scientific Instruments*, Vol. 73, 2001, pp. 1958-1961.

Zadrazil, I., Matar, O.K. and Markides, C.N., "An experimental characterization of downwards gas-liquid annular flow by laser-induced fluorescence: flow regimes and film statistics", *International Journal of Multiphase Flow*, Vol. 60, 2014, pp. 87–102.